Scientific Research Publishing

World Journal of Mechanics, 2023, 13, 93-105
https://www.scirp.org/journal/wjm
ISSN Online: 2160-0503
ISSN Print: 2160-049X

Dynamic Behavior of a Brushless in Runner Motor

Tièba Ouattara, Moussa Magara Traoré

Département de Génie Mécanique, Energétique et Mines, Ecole Normale d'Enseignement Technique et Professionnel (ENETP), Bamako, République du Mali
Email: ouat5tieba@gmail.com, mapatra@gmail.com

How to cite this paper: Ouattara, T. and Traoré, M.M. (2023) Dynamic Behavior of a Brushless in Runner Motor. *World Journal of Mechanics*, **13**, 93-105.
https://doi.org/10.4236/wjm.2023.134005

Received: March 30, 2023
Accepted: April 27, 2023
Published: April 30, 2023

Abstract

In this article, a model of a rotor with an asymmetric disk is presented in order to represent Campbell's diagrams and instability maps as a function of the rotations of the support which can significantly change the dynamic behavior of the rotor. Critical rotating speeds can also lead to unacceptable levels of vibration. Indeed, the critical speeds are a function of the dynamic rigidity of the rotating systems and the presence of the gyroscopic forces creates a dependence between the rotating speed of rotation and the natural frequencies to such structures (the CAMPBELL diagrams): this implies that the correct determination of the critical speeds is one of the essential elements when sizing such dynamic systems.

Keywords

Rotor Dynamics, Asymmetric Rotor, Parametric Excitation, Finite Element Method, Unbalance Response

1. Introduction

Spindles or rotors are defined as any element rotating around a fixed axis. They are used in many industrial applications and represent the centerpieces of rotating machines. Several studies of these systems have emerged, among which: The extended study of the dynamic behavior of a rotor mounted on a fixed support [1] [2]; the analysis of the stability of a beam whose equations of motion are parametric with periodic coefficients [3]; the stability and dynamic responses of a rotor with asymmetric geometry are studied [4] [5] [7]; studies relating to the dynamic behavior of on-board rotors under stresses [8], those of which the support is subjected to an earthquake [6] and to random stresses [8]. The works on on-board rotors interests us partially [9] [10].

Here we are interested in rotors whose supports are fixed as elucidated in some previous studies [11] [12] [13].

The spindle of a rotor can be considered as a continuous elastic body with properties of inertia and masses distributed along its length, especially in the high-speed range. Thus, vibrations appear in this mechanical system, limiting its performance and endangering its safety.

The dynamic analysis of continuous bodies in rotation makes it possible to understand their vibratory behaviors and to study their stabilities.

The objective of this work is to analyze the dynamic behavior of a brushless motor with elastic bearings and rigid and fixed supports.

The kinetic and strain energies as well as the virtual work of the components of the rotating flexible rotor are calculated. The proposed rotor model is based on the finite element method applied to a TIMOSHENKO beam. The use of the LAGRANGE equations provides the differential equations of the movement of the rotor in bending with fixed supports assumed to be rigid.

2. Material and Results

- **Basic theoretical model**

To analyze the dynamic behavior of a rotor whose support is fixed or subjected to any known movement, it is necessary to obtain the equations of the movement of the rotating system. The characteristics of each element of the rotor are determined. Thus, the expressions of the energies and of the virtual work corresponding to the basic elements (disc, spindle, bearing, unbalance) are determined.

The following Figure 1 is used to establish the equations of the different characteristics of a rotor bearing at both ends. These results will then be applied to a brushless inrunner motor.

- **Characteristics of the different elements of the model**
  - **Dynamic characteristics of the disc**
    - **Kinetic energy of the disc**

The disc is assumed to be rigid. Only its kinetic energy is considered.

Let $R_0(X_0, Y_0, Z_0)$ be a Galilean frame of reference (fixed) and $R(x, y, z)$ a main frame of inertia (rotating) linked to the disc (See Figure 2).

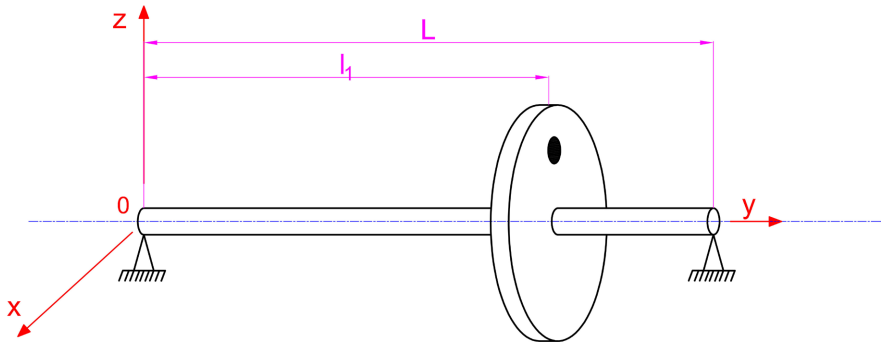

Figure 1. Basic theoretical model.

The coordinate system of the two reference marks are connected through the angles ψ, θ and ϕ (See Figure 3 for disc rotation details). The displacements along the axes $\overrightarrow{X_0}$ and $\overrightarrow{Z_0}$ are denoted respectively u and w. The displacement according to $\overrightarrow{Y_0}$ is supposed null because it is supposed that each point of the rotor moves in a plane perpendicular to $\overrightarrow{Y_0}$.

The general expression of the kinetic energy of the disk of mass m_d is:

$$T_d = \frac{1}{2} m_d \left\| \vec{V}_{R/R_0}(C) \right\|^2 + \frac{1}{2} {}^t\vec{\omega}_{R/R_0} \cdot I_c \cdot \vec{\omega}_{R/R_0} \tag{1}$$

With:

$$I_c = \begin{bmatrix} I_{dx} & 0 & 0 \\ 0 & I_{dy} & 0 \\ 0 & 0 & I_{dz} \end{bmatrix}_{(R)} \tag{2}$$

I_{dx}, I_{dy} and I_{dz} are the main moments of inertia of the disc following the directions $\overrightarrow{Ox}$, $\overrightarrow{Oy}$ and $\overrightarrow{Oz}$.

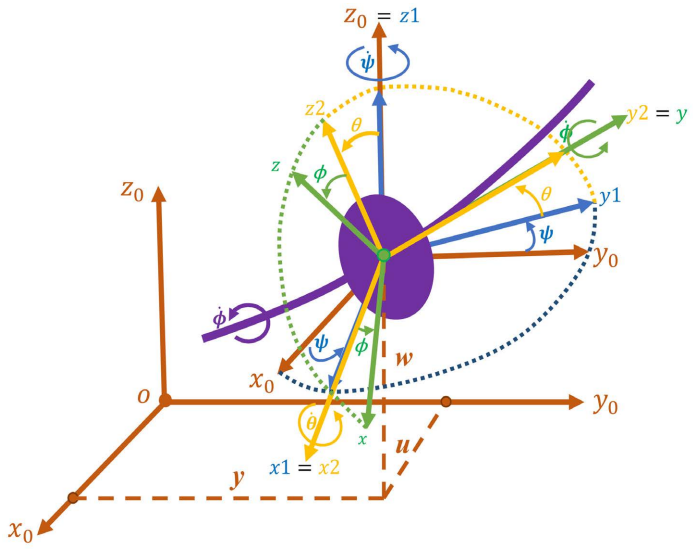

Figure 2. Reference marks of a disc mounted on a flexible rotating spindle.

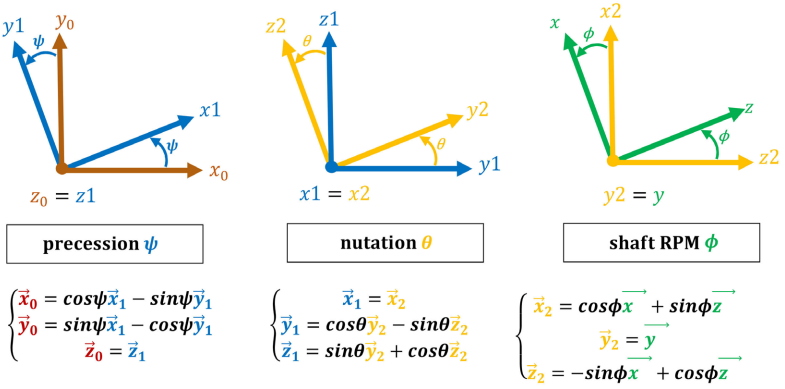

Figure 3. Details of the disc rotations (Euler's angles).

That is:

$$T_d = \frac{1}{2} m_d \left(\dot{u}^2 + \dot{w}^2 \right) + \frac{1}{2} \left(I_{dx} \omega_x^2 + I_{dy} \omega_y^2 + I_{dz} \omega_z^2 \right) \quad (3)$$

We can further simplify this expression by putting forward the following hypotheses: symmetrical disc, low bending of the spindle…

Thus, the kinetic energy of the disc is simplified to become:

$$T_d = \underbrace{\frac{1}{2} m_d \left(\dot{u}^2 + \dot{w}^2 \right)}_{\text{Translation}} + \underbrace{\frac{1}{2} I_{dx} \left(\dot{\theta}^2 + \dot{\psi}^2 \right)}_{\text{Rotation}} + \underbrace{I_{dy} \dot{\phi} \dot{\psi} \theta}_{\text{Effet Gyroscopique}} + \frac{1}{2} I_{dy} \dot{\phi}^2 \quad (4)$$

- **Dynamic characteristics of the Spindle**

The spindle is considered to be a beam of circular section, deformable and characterized by its kinetic and potential energies (of deformation).

➢ **Kinetic energy of the spindle**

The elementary kinetic energy $\mathrm{d}T_a$ of a spindle can be deduced by extending the kinetic energy of the disk by considering an infinitely thin spindle section of thickness $\mathrm{d}y$, of section S (assumed constant as show in Figure 4), of mass volume ρ_a and inertia of section I_{ax} and I_{az} (also assumed to be constant), In addition by taking as elementary mass: $\mathrm{d}m_a = \rho_a S \mathrm{d}y$ and as moments of inertia of the elementary mass $\mathrm{d}I_{ax}$ and $\mathrm{d}I_{az}$ in the reference $R(xyz)$; and finally with I_x and I_z as quadratic moments of inertia of the section of the elementary mass.

The elementary kinetic energy of an infinitely thin section of a spindle is then written:

$$\mathrm{d}T_a = \frac{1}{2} \mathrm{d}m_a \left(\dot{u}^2 + \dot{w}^2 \right) + \frac{1}{2} \left(\mathrm{d}I_{ax} \omega_x^2 + \mathrm{d}I_{ay} \omega_y^2 + \mathrm{d}I_{az} \omega_z^2 \right) \quad (5)$$

Considering that the cross sections of the beam are circular, the expression of the kinetic energy of the spindle is then obtained by integrating it over the entire length L:

$$T_a = \frac{\rho_a S}{2} \int_0^L \left(\dot{u}^2 + \dot{w}^2 \right) \mathrm{d}y + \frac{\rho_a I_s}{2} \int_0^L \left(\dot{\theta}^2 + \dot{\psi}^2 \right) \mathrm{d}y + 2 \rho_a I_s \dot{\phi} \int_0^L \theta \dot{\psi} \mathrm{d}y + \rho_a I_s L \dot{\phi}^2 \quad (6)$$

with:

$\frac{\rho_a S}{2} \int_0^L \left(\dot{u}^2 + \dot{w}^2 \right) \mathrm{d}y$: the expression of the kinetic energy of translation of a beam in bending.

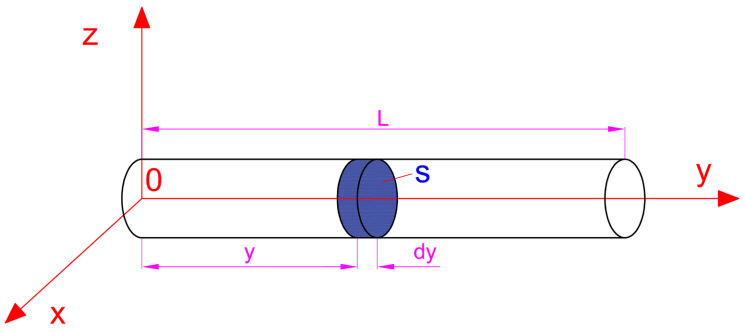

Figure 4. The flexible spindle with its infinitely thin elementary section.

$\frac{\rho_a I_s}{2}\int_0^L\left(\dot{\theta}^2+\dot{\psi}^2\right)\mathrm{d}y$: the side effect of the rotational energy of the spindle.

$2\rho_a I_s\dot{\varphi}\int_0^L\theta\dot{\psi}\mathrm{d}y$: the gyroscopic effect.

$\rho_a I_s L\dot{\varphi}^2$: the rotational energy of the spindle.

➢ **Spindle strain energy**

Considering a point B of the cross section of the spindle (Figure 5), u^* and w^* are the displacements of the geometric center C of the spindle along the x and z axes in the rotating frame, the displacements u^* and w^* are expressed in the fixed coordinate system.

The expression of the strain energy becomes:

$$U_a=\frac{E}{2}\int_0^L\int_s\left(-\frac{\partial\theta^*}{\partial y}z+\frac{\partial\psi^*}{\partial y}x\right)^2\mathrm{d}S\mathrm{d}y \tag{7}$$

And finally:

$$U_a=\frac{EI_s}{2}\int_0^L\left[\left(\frac{\partial^2 u}{\partial y^2}\right)^2+\left(\frac{\partial^2 w}{\partial y^2}\right)^2\right]\mathrm{d}y \tag{8}$$

- **Dynamic characteristics of the bearings**

In general, the bearings, considered to be non-rigid, induce external forces acting on the spindle. These stresses come from stiffness or damping as in [9] (Figure 6).

Les caractéristiques associées à ces efforts sont:

- k_{xx}, k_{zz}, c_{xx}, c_{zz} : stiffnesses and dampers according to the directions of the spindle X_0 et Z_0.
- k_{xz}, k_{zx}, c_{xz}, c_{zx} : stiffness and damping in one direction (X_0 or Z_0) but affected by the other direction; and represent mating constants.

The characteristics of stiffness and damping of the bearings are assumed to be known.

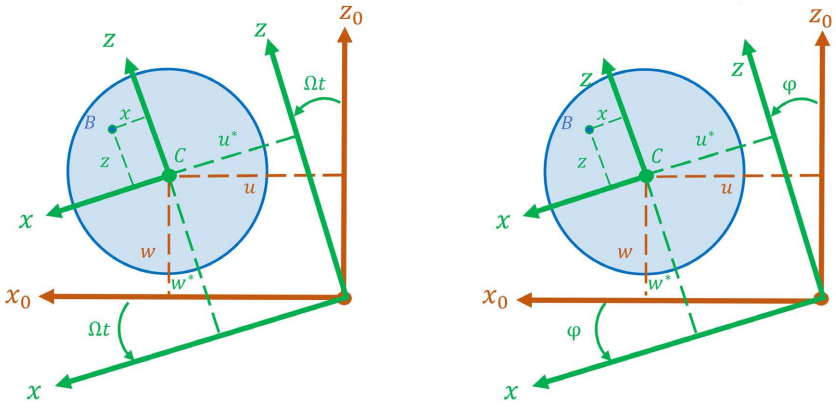

Figure 5. The displacement of the geometric center of the spindle: (a) for a constant speed of rotation of the spindle; (b) for a variable speed of rotation of the spindle.

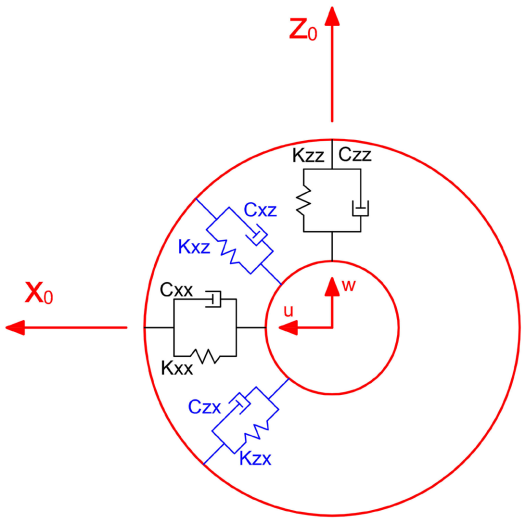

Figure 6. Damping and stiffness of the bearing.

$$\begin{bmatrix} F_u \\ F_w \end{bmatrix} = -\begin{bmatrix} K_{xx} & K_{xz} \\ K_{zx} & K_{zz} \end{bmatrix}\begin{bmatrix} u \\ w \end{bmatrix} - \begin{bmatrix} c_{xx} & c_{xz} \\ c_{zx} & c_{zz} \end{bmatrix}\begin{bmatrix} \dot{u} \\ \dot{w} \end{bmatrix} \tag{9}$$

where où F_u et F_w : the components of generalized forces.

The virtual work of these forces:

$$\delta w = F_u \delta u + F_w \delta w \tag{10}$$

- **Dynamic characteristics of the Unbalance:**

An unbalance is a quantity of matter located at a distance from the axis of rotation and capable of causing the appearance of centrifugal inertial forces. In our case, we will consider a single unbalance of mass m_b, located at point B in the plane of the disc (xOz) at a distance d from its geometric center C (**Figure 7**).

Kinetic energy of unbalance:

$$T_b = \frac{1}{2} m_b \left[\dot{u}^2 + \dot{w}^2 + d^2\dot{\varphi}^2 + 2\dot{u}d\dot{\varphi}\cos\varphi - 2\dot{w}d\dot{\varphi}\sin\varphi \right] \tag{11}$$

$\dot{u}^2$ et $\dot{w}^2$ being negligible, then we have:

$$T_b = \frac{1}{2} m_b \left[d^2\dot{\varphi}^2 + 2\dot{u}d\dot{\varphi}\cos\varphi - 2\dot{w}d\dot{\varphi}\sin\varphi \right] \tag{12}$$

o **Brushless motor spindle modeling**

Here (in **Figure 8**) we will use the model studied by Lalanne/Ferraris [1] and adapt it to an experimental brushless inrunner motor as in [9].

The rotor characteristics are as follows:

➢ *For the disc*:

- Internal radius R_{d1} = 0.001 m
- External radius R_{d2} = 0.015 m
- Thickness h = 0.03 m
- Density: $\rho_d = \rho$ = 7800 kg/m^3
- Young modulus: $E_d = E$
- Position: $l_1 = L/3$

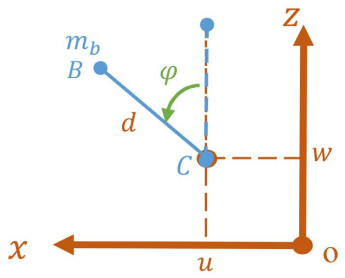

Figure 7. The unbalance.

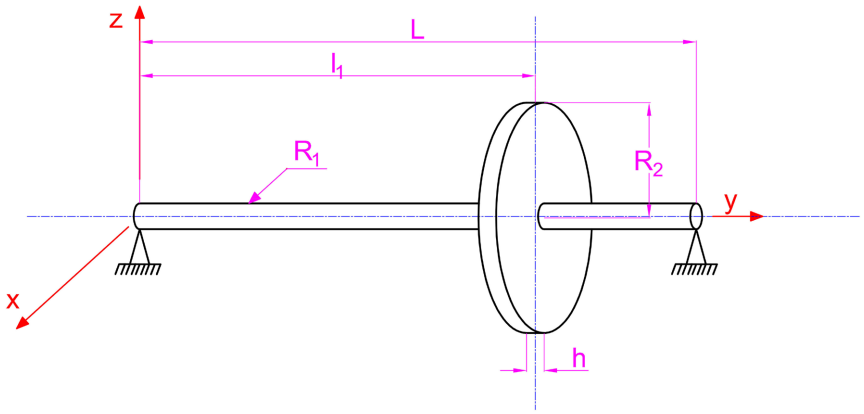

Figure 8. The spindle schematic of the brushless in runner motor.

- Mas $m_d = \pi\rho\left(R_{d2}^2 - R_{d1}^2\right)h = 1.65\times10^{-1}$ kg
- Inertias: $I_{dx} = I_{dz} = \dfrac{m_d}{12}\left(3R_{d1}^2 + 3R_{d2}^2 + h^2\right) = 2.17\times10^{-5}\ \text{kg}\cdot\text{m}^2$

$$I_{dy} = \frac{m_d}{2}\left(R_{d1}^2 + R_{d2}^2\right) = 1.86\times10^{-5}\ \text{kg}\cdot\text{m}^2$$

➢ *For the spindle*:

- Length $L = 0.05$ m
- cross-section radius $R_a = 0.001$ m
- $\rho = 7800$ kg/m^3
- $E = 2\times10^{11}$ Pa
- Area of the cross-section $S = \pi R_a^2 = 3.142\times10^{-6}\ \text{m}^2$
- Quadratic moment of inertia $I_s = \dfrac{\pi R_a^2}{2} = 1.57\times10^{-12}\ \text{m}^4$.
- *For unbalance*:
- Mass $m_b = 10^{-4}$ kg
- Distance $d = 0.02$ m
- *For the bearing*:
- Stiffness $k_{xx} = 0$ et $k_{zz} = 0$

The behavior of the spindle is that of the first mode of a beam in bending, of constant section and in support at both ends (**Figure 9**):

$$f(y) = \sin\frac{\pi y}{L} = \sin\frac{\pi y}{0.05} = \sin 62.83y$$

The total kinetic energy T is given by:

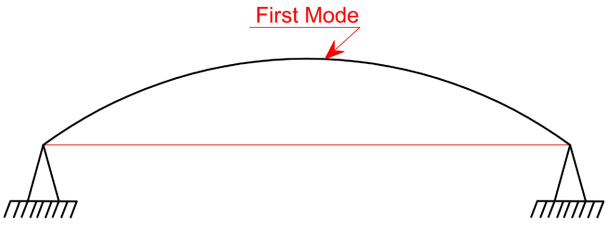

Figure 9. The first mode of vibration.

$$T = T_a + T_d + T_b \tag{13}$$

$$\begin{aligned} T = &\left[\frac{1}{2}\rho_a S_a \int_0^L \left(\dot{u}^2 + \dot{w}^2\right) \mathrm{d}y + \frac{1}{2}\rho_a I_s \int_0^L \left(\dot{\psi}^2 + \dot{\theta}^2\right) \mathrm{d}y + 2\rho_a I_s \dot{\varphi} \int_0^L \dot{\psi}\theta \mathrm{d}y + \rho_a I_s L \dot{\varphi}^2\right] \\ &+ \left[\frac{1}{2} m_d \left(\dot{\psi}^2 + \dot{\theta}^2\right) + \frac{1}{2} I_{dx} \left(\dot{\psi}^2 + \dot{\theta}^2\right) + \frac{1}{2} I_{dy} \left(2\dot{\varphi}\dot{\psi}\theta + \dot{\varphi}^2\right)\right] \\ &+ \frac{1}{2} m_b \left[d^2 \dot{\varphi}^2 + 2\dot{u} d \dot{\varphi} \cos\varphi - 2\dot{w} d \dot{\varphi} \sin\varphi\right] \end{aligned} \tag{14}$$

By replacing the following expressions with their values:

$$\begin{aligned} &w(y,t) = f(y) q_2(t); \dot{w}(y,t) = f(y) \dot{q}_2(t) \\ &\psi(y,t) = -g(y) q_1(t); \dot{\psi}(y,t) = -g(y) \dot{q}_1(t) \\ &\theta(y,t) = g(y) q_2(t); \dot{\theta}(y,t) = g(y) \dot{q}_2(t) \end{aligned} \tag{15}$$

Kinetic energy will be written as:

$$T = \boldsymbol{a}\left(\dot{q}_1^2 + \dot{q}_2^2\right) - \dot{\varphi}\boldsymbol{b}\dot{q}_1 q_2 + \dot{\varphi}\boldsymbol{c}\left(\dot{q}_1 \cos\varphi - \dot{q}_2 \sin\varphi\right) + Cste \tag{16}$$

The strain energy is given by:

$$U = \frac{1}{2} E_a I_s \int_0^L \left[\left(\frac{\partial^2 u}{\partial y^2}\right)^2 + \left(\frac{\partial^2 w}{\partial y^2}\right)^2\right] \mathrm{d}y \tag{17}$$

By replacing the following expressions with their values:

$$\frac{\partial^2 u}{\partial y^2} = h(y) q_1(t); \quad \frac{\partial^2 w}{\partial y^2} = h(y) q_2(t) \tag{18}$$

$$U = \boldsymbol{d}\left(q_1^2 + q_2^2\right) \tag{19}$$

Apply the Lagrange equation:

$$\frac{\mathrm{d}}{\mathrm{d}t}\left(\frac{\partial T}{\partial \dot{q}_i}\right) - \frac{\partial T}{\partial q_i} + \frac{\partial U}{\partial q_i} = F_{q_i} \tag{20}$$

There will be the following system:

$$\begin{cases} 2a\ddot{q}_1 - b\dot{\varphi}\dot{q}_2 + 2dq_1 - \ddot{\varphi}bq_2 = c\dot{\varphi}^2 \sin\varphi + c\ddot{\varphi}\cos\varphi \\ 2a\ddot{q}_2 - b\dot{\varphi}\dot{q}_1 + 2dq_2 = c\dot{\varphi}^2 \cos\varphi + c\ddot{\varphi}\sin\varphi \end{cases} \tag{21}$$

Conditions:

- Constant speed

$$\varphi = \Omega t \quad \text{et} \quad \dot{\varphi} = \Omega, \text{ alors} \quad \ddot{\varphi} = 0 \tag{22}$$

➢ And with:

$$2a = m;\ \ b = \beta \quad \text{et} \quad 2d = k \tag{23}$$

The general form will be:

$$\begin{cases} m\ddot{q}_1 - \beta\Omega\dot{q}_2 + kq_1 = c\Omega^2 \sin\Omega t \\ m\ddot{q}_2 + \beta\Omega\dot{q}_1 + kq_2 = c\Omega^2 \cos\Omega t \end{cases} \tag{24}$$

The natural frequency is determined for the two possible cases (rotor stopped and rotor rotating)

- Rotor stopped ($\Omega = 0$):

$$\omega_{01} = \omega_{02} = \omega_0 = \sqrt{\frac{k}{m}} \tag{25}$$

- Rotor rotating ($\Omega \neq 0$):

$$\omega_1 = \sqrt{\omega_0^2 + \frac{\beta^2\Omega^2}{2m^2}\left(1 - \sqrt{1 + \frac{4m^2\omega_0^2}{\beta^2\Omega^2}}\right)} \tag{26}$$

$$\omega_2 = \sqrt{\omega_0^2 + \frac{\beta^2\Omega^2}{2m^2}\left(1 + \sqrt{1 + \frac{4m^2\omega_0^2}{\beta^2\Omega^2}}\right)} \tag{27}$$

with:

$$\omega_0^2 = \frac{k}{m} \quad \text{et} \quad m^2\omega_0^2 = km \tag{28}$$

To each of the values ω_1 and ω_2 corresponds a mode:

• When $\omega = \omega_1$ et $\omega_1 < \omega_0$ (1^{st} mode):

The movement along the $\overrightarrow{Ox}$ axis is π/2 ahead of the movement along the *Oz* axis but have the same amplitudes. These points turn in the opposite direction of the rotation of the rotor so we say that we have a reverse or retrograde precession as in [13] **Figure 10**.

• When $\omega = \omega_2$ et $\omega_2 > \omega_0$ (2^{nd} mode):

The following movement $\overrightarrow{Ox}$ is late compared to the movement according to $\overrightarrow{Oz}$ of π/2, but they have the same amplitudes. We say in this case that we have a direct precession as in [13] **Figure 11**.

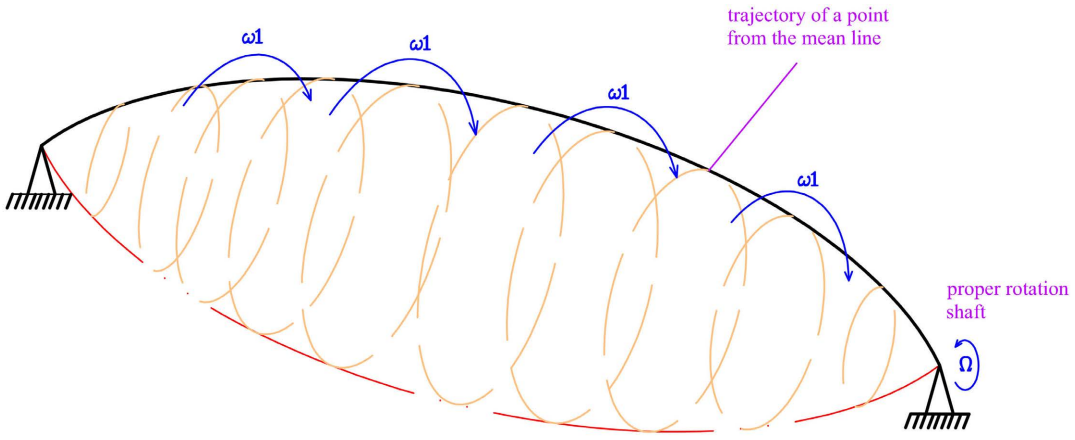

Figure 10. Reverse precession.

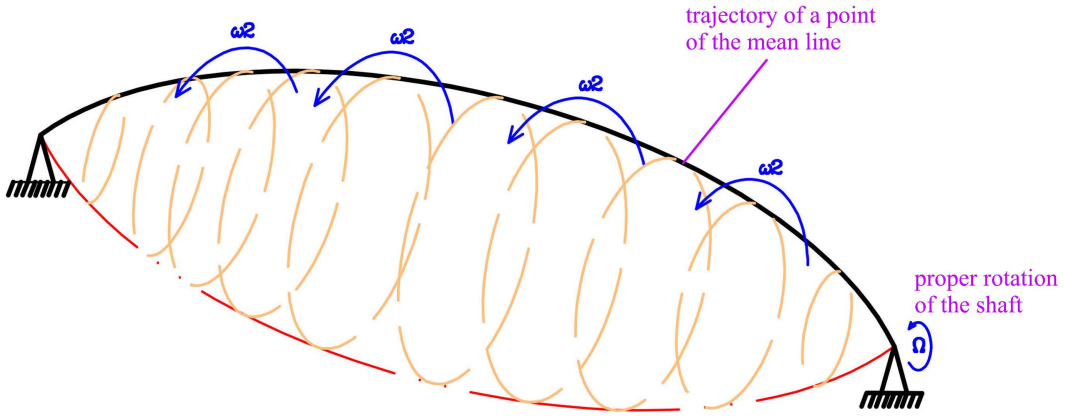

Figure 11. Direct precession.

Using data from the symmetrical rotor of our Motor:

- The equation of the system becomes:

$$\begin{cases} 1.32\times10^{-1}\ddot{q}_1 - 1.84\times10^{-2}\Omega\dot{q}_2 + 1.22\times10^{5}q_1 = 1.73\times10^{-6}\Omega^2\sin\Omega t \\ 1.32\times10^{-1}\ddot{q}_2 + 1.84\times10^{-2}\Omega\dot{q}_1 + 1.22\times10^{5}q_2 = 1.73\times10^{-6}\Omega^2\cos\Omega t \end{cases} \quad (29)$$

The natural frequencies when stopped are:

$$\omega_{10} = \omega_{20} = \omega_0 = 961\,\text{rds/s} \quad (30)$$

The natural frequencies in rotation are:

$$\omega_1 = \sqrt{9.24\times10^{5} + 9.72\times10^{-3}\Omega^2\left(1 - \sqrt{1 + \frac{1.90\times10^{8}}{\Omega^2}}\right)} \quad (31)$$

$$\omega_2 = \sqrt{9.24\times10^{5} + 9.72\times10^{-3}\Omega^2\left(1 + \sqrt{1 + \frac{1.90\times10^{8}}{\Omega^2}}\right)} \quad (32)$$

Campbell's diagrams (**Figure 12** and **Figure 13**) represent the resonant frequencies of the rotor as a function of the rotational speeds:

With Campbell's diagram, the functions $\omega_1 = \omega_1(\Omega)$ and $\omega_2 = \omega_2(\Omega)$ are cut by the lines $\omega = \Omega$ (synchronous case) and $\omega = s\Omega$ (asynchronous case) which gives points of intersections A and B for the first, and C and D for the second (C and D does not exist on our diagram because there is no asynchronous case). Ω10, which is the point of intersection of curves ω_1 (direct mode) and ω_2 (indirect or retrograde mode) is the resonant frequency of the rotor at standstill. A and B are the points at which the rotational speed of the rotor coincides with its resonant frequencies.

- **The Resonant Amplitudes:**

By considering the centrifugal force of the unbalance (2nd member):

$$\begin{cases} m\ddot{q}_1 - \beta\Omega\dot{q}_2 + kq_1 = c\Omega^2\sin\Omega t \\ m\ddot{q}_2 + \beta\Omega\dot{q}_1 + kq_2 = c\Omega^2\cos\Omega t \end{cases} \quad (33)$$

Solutions are in the form:

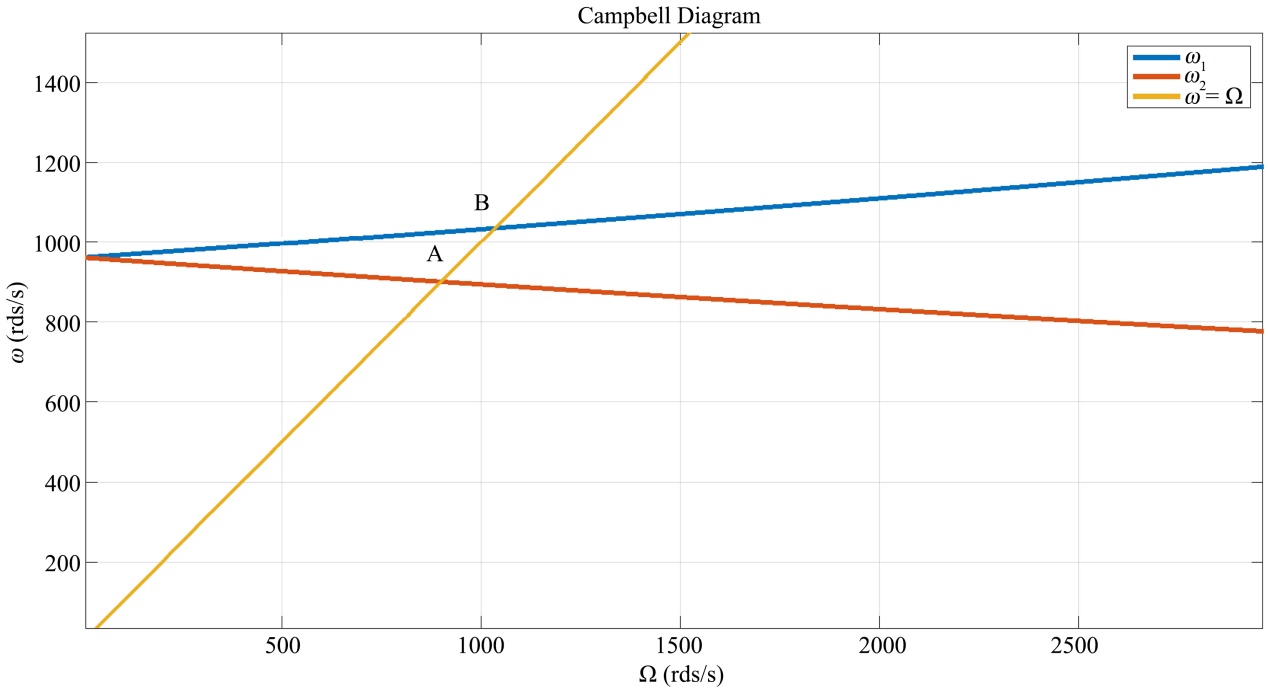

Figure 12. This diagram allows us to see the pulsation for which the system enters into resonance.

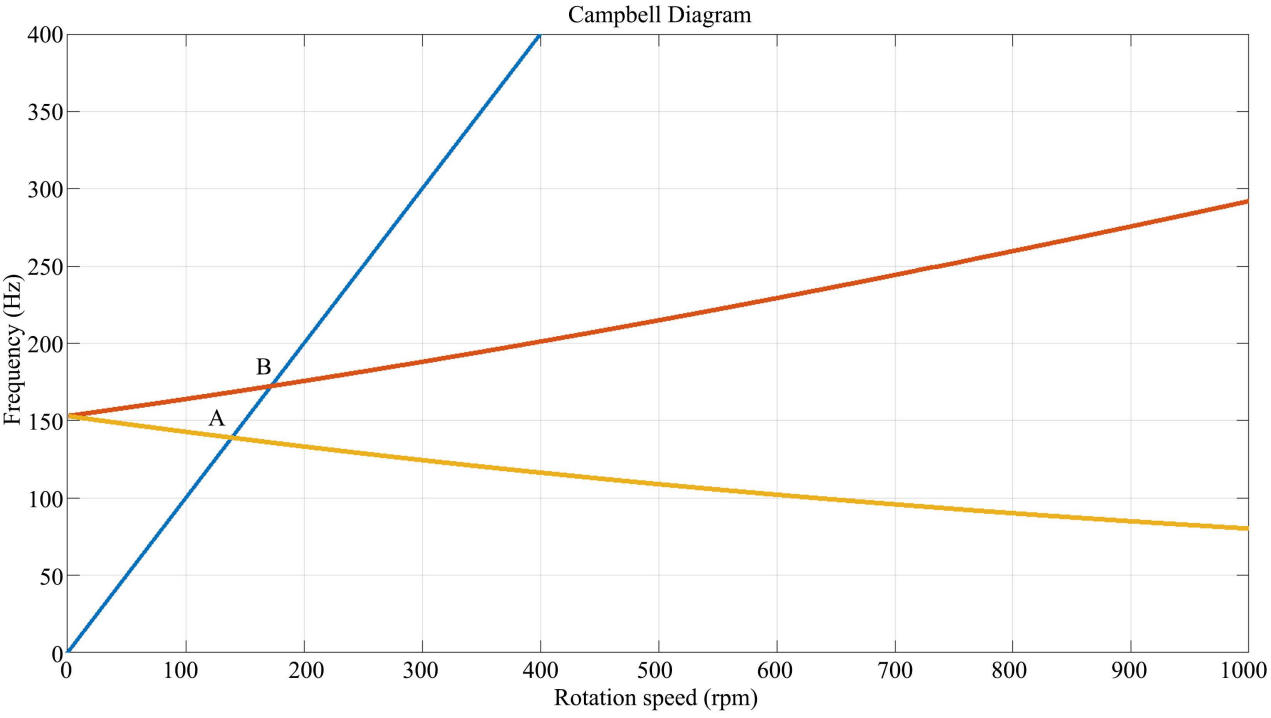

Figure 13. This diagram allows us to see the speed of rotation causing the resonance frequency.

$$\begin{cases} \overline{q}_{1p} = \overline{A}_{e1} e^{j\Omega t} \\ \overline{q}_{2p} = \overline{A}_{e2} e^{j\Omega t} \end{cases} \tag{34}$$

With $\overline{A}_{e1} = A_{e1} e^{j\Phi_{e1}}$ et $\overline{A}_{e2} = A_{e2} e^{j\Phi_{e2}}$

Then $\Phi_{e1} = -\frac{\pi}{2}$ et $\Phi_{e2} = 0$

Thus $A_{e1} = A_{e2}$; so the orbits described by the rotor are circles.

$$A_{e1} = A_{e2} = \frac{c\Omega^2\left(k - m\Omega^2 - \beta\Omega^2\right)}{\left(k - m\Omega^2\right)^2 - \beta^2\Omega^4} \tag{35}$$

Note that this function has a limit of $\frac{c}{m-\beta}$ when Ω tends to infinity

The critical speed of a rotor subjected to an unbalance corresponds to the value of Ω for which the displacement is infinite. That is, when the denominator is equal to 0.

$$\Omega_c = \sqrt{\frac{k}{m-\beta}} \tag{36}$$

This value corresponds to point B of the Campbell diagram because of the influence of the stiffness symmetries of the bearings

3. Conclusion

The model developed with the Rayleigh-Ritz method is used in this study because of its simplicity. It sets up a model making it possible to treat simple cases and to highlight basic phenomena. It consists in replacing the unknown field by a finite number of unknown coefficients, which results in a field of displacements smaller than the exact solution. So, the approximate model is more rigid than the exact model. Finally, she uses few degrees of freedom to write the equations of motion. This allows us to quickly have information on the dynamic behavior of the rotor, with little precision. Thus, to avoid high amplitude responses that can lead to their destruction, the natural frequencies of the system must be distinct from the excitation frequencies throughout the operating range. For this, the critical speed was determined using the Campbell diagram; which is to be avoided, so as not to cause the resonance of the system. Technically, this speed is quickly exceeded by the engine when starting, to reach the operating range which is beyond 1000 rpm.

Conflicts of Interest

The authors declare no conflicts of interest regarding the publication of this paper.

References

[1] Lalanne, M. and Ferraris, G. (1998) Rotordynamics Prediction in Engineering. Wiley, Chichester.

[2] Genta, G. (2005) Dynamics of Rotating Systems. Springer, New York. https://doi.org/10.1007/0-387-28687-X

[3] Dufour, R. and Berlioz, A. (1998) Parametric Instability of a Beam Due to Axial Excitations and to Boundary Conditions. *ASME Journal of Vibration and Acoustics*, **120**, 461-467. https://doi.org/10.1115/1.2893852

[4] Guilhen, P.M., Berthier, P., Ferraris, G. and Lalanne, M. (1988) Instability and Unbalance Response of Dissymmetric Rotor-Bearing Systems. *ASME Journal of Vibration, Acoustics, Stress and Reliability in Design*, **110**, 288-294. https://doi.org/10.1115/1.3269515

[5] Kang, Y., Shih, Y.-P. and Lee, A.-C. (1992) Investigation on the Steady-State Responses of Asymmetric Rotors. *ASME Journal of Vibration and Acoustics*, **114**, 194-208. https://doi.org/10.1115/1.2930249

[6] Beley-Sayettat, A. (1994) Effet des Dissymétries et Effet Sismique en Dynamique des Rotors. Thèse LMSt. INSA de Lyon, Lyon.

[7] Oncescu, F., Lakis, A.A. and Ostiguy, G. (2001) Investigation of the Stability and Steady State Response of Asymmetric Rotors, Using Finite Element Formulation. *Journal of Sound and Vibration*, **245**, 303-328. https://doi.org/10.1006/jsvi.2001.3570

[8] Bachelet, L., Driot, N. and Ferraris, G. (2006) Comportement dynamique des rotors embarqués sous sollicitations aléatoires. *XV Colloque Vibrations*, Chocs et Bruits, Lyon, 14-16 June 2006.

[9] Duchemin, M. (2003) Contribution à l'étude du comportement dynamique d'un rotor embarqué. Ecole doctorale des sciences pour l'ingenieur de lyon, Lyon.

[10] Zaki Dakel, M. (2014) Stabilité et dynamique non linéaire de rotor embarqués. INSA de Lyon.

[11] Boukhalfa, A. (2009) Comportement vibratoire des arbres tournants en matériaux composites. Universite Abou Bekr Belkaid, Tlemcen.

[12] Guillaume, M. (2011) Identification et prévision du comportement dynamique des rotors feuilletés en flexion. INSA de Lyon.

[13] Medour, M. (2019) Dynamique de machines tournantes: 2ème Année Master, Construction Mecanique.